Two distinct glutamatergic synaptic inputs to striatal medium spiny neurones of neonatal rats and paired-pulse depression

Akihisa Mori, Tetsuo Takahashi*, Yasushi Miyashita and Haruo Kasai†

*Department of Physiology, Faculty of Medicine, University of Tokyo, Hongo, Bunkyo-ku, Tokyo 113, Japan and *Department of Molecular Neurobiology, School of Human Science, Waseda University, Mikajima, Saitama 359, Japan*

1. Excitatory postsynaptic currents (EPSCs) were recorded from the medium spiny neurones of neonatal rat striatal slices using the whole-cell patch clamp method. EPSCs were selectively elicited in the presence of picrotoxin with a glass stimulating pipette placed in the striatum.

2. We found two distinct unitary EPSCs that were evoked by stimulation of single presynaptic fibres. The major type of EPSC, termed 'S-type', failed frequently and had a small mean amplitude (2·05 pA). They probably represented cortical afferents.

3. The other type of unitary EPSC, the 'H-type', seldom failed and was 13 times larger than the S-type. Spontaneous EPSCs with amplitudes similar to those of H-type EPSCs could be induced.

4. H-type EPSCs were mediated by both non-NMDA and NMDA receptors.

5. The two types of EPSCs could be evoked in the same neurones. The intensity of stimulation for H-type EPSCs was higher than that for S-type EPSCs.

6. H-type EPSCs could be polysynaptically activated, suggesting the presence of glutamatergic interneurones in the striatum that generated H-type EPSCs.

7. H-type EPSCs displayed particularly long-lasting paired-pulse depression, while that displayed by the S-type EPSCs was short. The paired-pulse depression of both EPSCs was Ca^{2+} dependent and involved presynaptic mechanisms.

8. We have demonstrated that the medium spiny neurones of neonatal rats receive two different glutamatergic input systems having different amplitudes, origins and paired-pulse depression, reminiscent of cerebellar Purkinje cells. This suggests that the two types of EPSCs also play distinctive roles in striatal neuronal circuitry.

Many aspects of synaptic organization of the striatum remain unexplored compared with another subcortical motor centre, the cerebellum. The principal neurones in the striatum are medium-sized neurones heavily laden with spines, and hence usually referred to as the medium spiny neurones. These neurones receive glutamatergic inputs from the cerebral cortex and thalamus, and send GABAergic axons to the globus pallidus and substantia nigra (Graybiel, 1990; Gerfen, 1992). The principal neurones comprise 90–95% of the neuronal population in the striatum: the remainder of neurones are considered interneurones. There are two major classes of interneurones; one is the cholinergic giant aspiny neurones (Bolam, Wainer & Smith, 1984), and the other comprises several types of medium aspiny neurones, whose transmitters have only partly been clarified (DiFiglia & Aronin, 1982; Bolam, Clark, Smith & Somogyi, 1983; Takagi, Somogyi, Somogyi & Smith, 1983; Vincent & Johansson, 1983; Oertel & Mugnaini, 1984). Anatomical studies have indicated the presence of mutual connections between these three classes of neurones; however, none of them has been characterized physiologically (Gerfen, 1992). Moreover, the way in which a single cortical afferent affects individual medium spiny neurones has not been elucidated. The lack of fundamental physiological knowledge has hampered the understanding of striatal functions. It is difficult to examine the synaptic organization of the striatum because of its anatomical organization. All neuronal types are homogeneously mixed and hence stimulation of specific presynaptic fibres is difficult. This marks a clear contrast with studies of the cerebellum, where the segregated localization of five major types of neurones has assisted in characterization of mutual synaptic connections (Eccles, Ito & Szentágothai, 1967), and a

† To whom correspondence should be addressed.

concrete model for its operation has been proposed (Marr, 1969; Albus, 1971) and experimentally tested (Ito, 1984).

In an attempt to reinforce our knowledge of the synaptic organization of the striatum, we have examined excitatory inputs to the medium spiny neurones, making use of the whole-cell patch clamp recording technique in thin-slice preparations. Our strategy was to characterize each specific input by stimulating single presynaptic fibres. Fine glass pipettes were therefore used to stimulate a small part of the striatum close to recorded cells, and intensities of stimuli were carefully adjusted. We found that the unitary EPSCs were classified into two types with widely different amplitudes. One type exhibited particularly long-lasting paired-pulse depression, strongly supporting the possibility that the two EPSCs arose from distinct synapses. Our results further suggested that the two types of EPSCs arose from different presynaptic cells, the cortical pyramidal cells and striatal interneurones. Therefore, we concluded that the glutamatergic input system of the striatal medium spiny neurones bears a similarity to that of cerebellar Purkinje cells (Eccles *et al.* 1967) in that both neurones receive two distinctive glutamatergic inputs with different amplitudes coming from different brain areas. Preliminary results of these experiments have been reported in abstract form (Mori, Takahashi, Miyashita & Kasai, 1992).

METHODS

Preparation of slices

Young Wistar rats (9–14 days old) were decapitated and their forebrains were quickly removed. Thin horizontal slices 150–220 μm in thickness were obtained from the striatum with a vibratome. Our slices included only the striatum and neocortex. The slices were incubated for more than 1 h in a normal slice solution composed of 120 mM NaCl, 3 mM KCl, 2·5 mM $CaCl_2$, 1·2 mM $MgCl_2$, 23 mM $NaHCO_3$, 1·5 mM Na_2PO_3, 11 mM glucose, and oxygenated with 95 % O_2 and 5 % CO_2 at 32 °C. For electrophysiological experiments, the slices were transferred to a recording chamber, where oxygenated normal slice solution containing picrotoxin (0·1 mM; Wako Pure Chemical, Japan) was continuously superfused at room temperature (23–26 °C).

Patch clamping

Whole-cell clamp experiments were performed, directly visualizing cells using an upright Nomarski microscope with a ×40 water immersion objective (Optiphoto; Nikon, Japan). We chose only small neurones with diameters of less than 13 μm; hence, most of the recorded neurones should have been the medium spiny neurones. Injection of Lucifer Yellow (Sigma, USA) revealed some features of the neurones. The cells projected several fine dendrites, 100–250 μm long, in all directions. Fine spiny structures were often visualized, particularly when cells were located close to the surface.

Edwards, Konnerth, Sakmann & Takahashi (1989) reported a cleaning procedure used to assist in the formation of a giga-seal in thin-slice preparations. However, we found that this procedure always damaged the medium spiny cells, presumably because it tended to damage one of their dendrites. To form a giga-seal, we applied positive pressure to the patch pipette while it was inserted into slices. When the tip of the pipette was apposed to the surface of a cell, a strong positive pressure was applied once to clean the cell's surface, and then weak suction was applied to achieve the giga-seal. The pipette solution contained 120 mM caesium gluconate, 10 mM CsCl, 2 mM $MgCl_2$, 0·5 mM ATP, 10 mM NaHepes, and 0·5 mM CsEGTA at pH 7·2. The resistances of the patch pipettes using this solution ranged from 6 to 12 MΩ, and series resistances measured during the whole-cell configuration ranged from 20 to 45 MΩ. The liquid junction potential between the pipette and recording solutions was estimated as −10 mV ($n = 6$; Neher, 1992). Cells were held at −70 mV, taking into account this liquid junction potential. Stable recordings with leak currents of less than 100 pA could be achieved for up to 20 min. It was, however, very difficult to maintain a good seal at holding potentials more negative than −70 mV. Stimulation of afferent fibres was performed using a glass micropipette with a tip diameter of 5 μm. The stimulation electrodes were filled with the external solution. Rectangular voltage pulses with amplitudes between 8 and 30 V and a duration of 200 μs were applied to the glass pipette relative to a reference electrode placed in the recording chamber. EPSCs were evoked every 5–10 s. A low-Ca^{2+} solution and the normal recording solutions containing either 6-cyano-7-nitroquinoxaline-2,3-dione (CNQX; Tocris, UK) or 2-amino-5-phosphonovalerate (APV; Sigma, USA) were superfused through the recording chamber.

All current records were filtered at 1 kHz, sampled at 10 kHz, and relayed to a digital computer (98DS; NEC, Japan). Stimulation artifacts were reduced by subtracting either the averaged current traces in which EPSCs failed or averaged current traces evoked at 0 mV. The peak amplitudes of the EPSCs were calculated using the computer as follows. (1) Moving averages with a time window of 2 ms were calculated at two periods, 2–7 ms before and after the stimulation. (2) Differences between the minimum values in the two periods were taken as peak amplitudes of EPSCs. Latencies and times to peak of EPSCs were estimated visually with the aid of computer graphics. Amplitude histograms were fitted with a sum of Gaussian functions by the maximum-likelihood method as described by Edwards, Konnerth & Sakmann (1990).

RESULTS

S-type EPSCs

Excitatory postsynaptic currents (EPSCs) were recorded from medium spiny neurones in the presence of picrotoxin, while stimulating the surface of the thin striatal slices using a glass electrode placed within 200 μm of the recording electrode. The EPSCs were mediated by glutamate receptors; the major fast components were eliminated with CNQX (10 μM), and the remaining slow components, prominent at positive membrane potentials, were eliminated by APV (0·3 mM), consistent with a previous study (Jiang & North, 1991).

To evoke the unitary EPSCs that were generated by a single presynaptic fibre, stimulus intensities were finely adjusted, as illustrated in Fig. 1*A*. Since the amplitudes of

the EPSCs displayed considerable fluctuation (uppermost trace in Fig. 1*A*), the mean amplitude of ten consecutive EPSCs was also plotted, as shown in the middle trace of Fig. 1*A*. As stimulus intensity (lowermost trace in Fig. 1*A*) was reduced from 20·5 to 17·5 V (indicated by the dotted line between periods *a* and *b* in Fig. 1*A*), the mean amplitude declined. Between 17·5 and 15 V, however, there was virtually no systematic change in the mean amplitudes (periods *b* and *d*). The EPSCs suddenly disappeared at 14·5 V (period *c*). These data suggest that only one presynaptic fibre was stimulated when the stimuli ranged between 15 and 17·5 V, and more than one fibre was stimulated with stimuli larger than 17·5 V. Based on these findings, a total of 158 unitary EPSCs were evoked at 16 V (Fig. 1*B*), and amplitude histograms were constructed (Fig. 1*C*). The amplitude histograms could be fitted with the sum of two Gaussian distributions. One peak apparently represented transmission failure (Fig. 1*C*), because it was similar to the amplitude histogram obtained at the end of the current traces where currents recovered to baseline levels (Fig. 1*D*). The other component corresponded to the net amplitude distribution for the EPSCs. This net amplitude distribution peaked at 4·05 pA with a larger standard deviation (S.D., 1·95 pA) than that of the baseline noise level (0·99 pA, Fig. 1*D*). The latency histogram showed a single sharp peak 3 ms after the onset of stimulation (Fig. 1*E*), supporting the hypothesis that these EPSCs were monosynaptic and evoked by stimulation of a single presynaptic fibre. The times to peak of the EPSCs showed some variability (Fig. 1*F*), and were not correlated with the amplitudes of EPSCs (Fig. 1*G*). Similar analysis was performed in twenty-eight synapses, and this type of small and single-peaked amplitude distribution was found in sixteen synapses. We will call unitary EPSCs of this

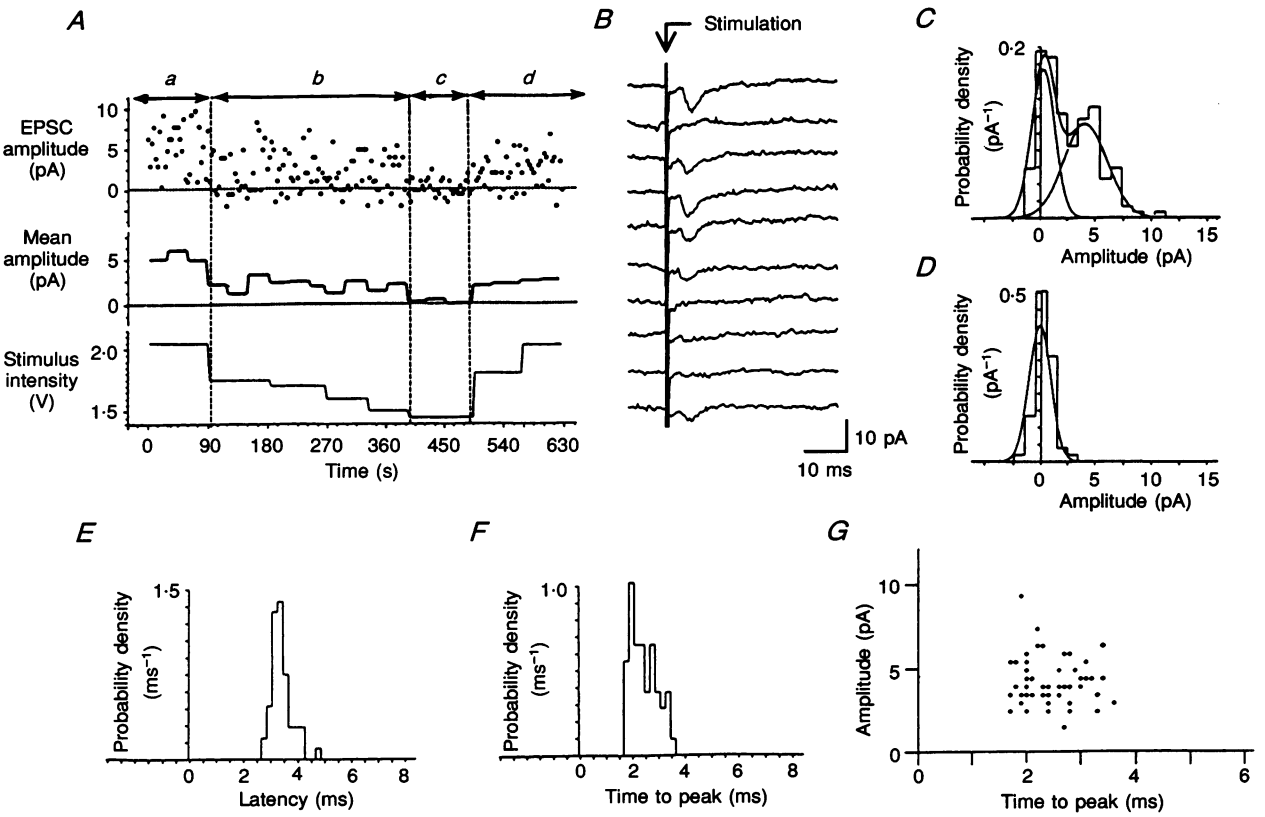

Figure 1. Unitary S-type EPSCs recorded from a medium spiny neurone in the striatum
A, changes in amplitudes of EPSCs (uppermost trace) evoked by stimuli with varying intensities (lowermost trace). The middle trace shows the average amplitude of 10 consecutive EPSCs. In the period designated by *a*, multiple fibres were stimulated, while in *b* and *d*, a single fibre was stimulated, and in *c*, no fibres were stimulated. *B*, examples of unitary EPSCs were elicited consecutively with a constant stimulus at 16 V. These EPSCs were recorded after the period *d* in *A*. *C*, amplitude histogram constructed from 158 of such EPSCs. Curves represent the best fit of the histogram with a sum of two Gaussian distributions. The mean and weight of the net EPSC component were 4·05 pA and 0·54, respectively. *D*, amplitude histogram obtained from the same current traces as used in *C* but at the end of the traces. *E*, latency histogram. *F*, time-to-peak histogram. *G*, correlation between times to peak and amplitudes of EPSCs. No correlation was observed (correlation coefficient = 0·059). In *E–G*, $n = 54$. For simplicity, the sign of the current is inverted in all amplitude and correlation plots in Figs 1–6.

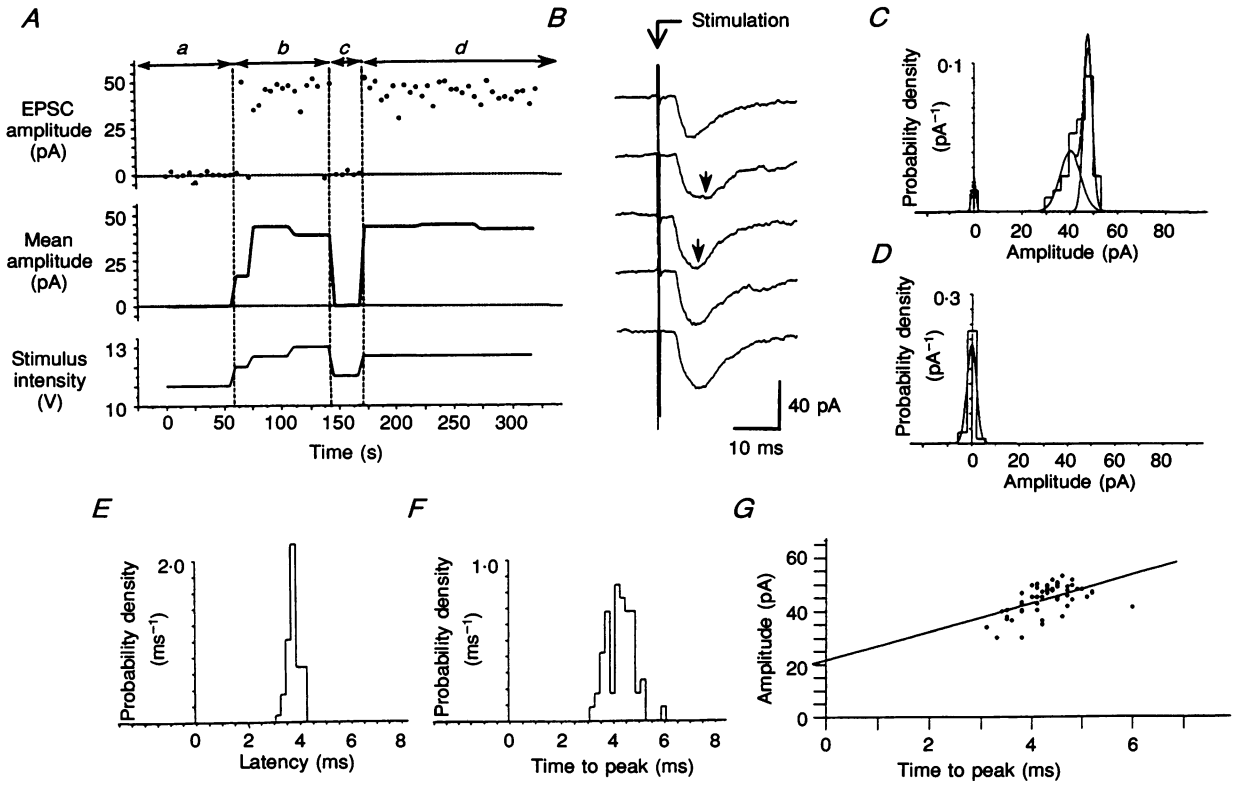

Figure 2. Unitary H-type EPSCs in a medium spiny neurone
A, changes in amplitudes of EPSCs (uppermost trace) evoked with different intensities of stimuli (lowermost trace). Mean amplitude of 10 consecutive EPSCs is shown in the middle panel. *B*, unitary H-type EPSCs consecutively evoked at 12·5 V. Arrows indicate delayed peaks. *C* and *D*, amplitude histograms for 61 EPSCs (*C*) and for noise (*D*). The amplitude of the largest peak was 47·4 pA in *C* and 0·2 pA in *D*. *E*, latency histogram. *F*, time-to-peak histogram. *G*, correlation between times to peak and amplitudes of EPSCs. There is clear correlation (correlation coefficient = 0·543, $P < 0·05$). A straight line shows the result of linear regression. In *E–G*, $n = 59$.

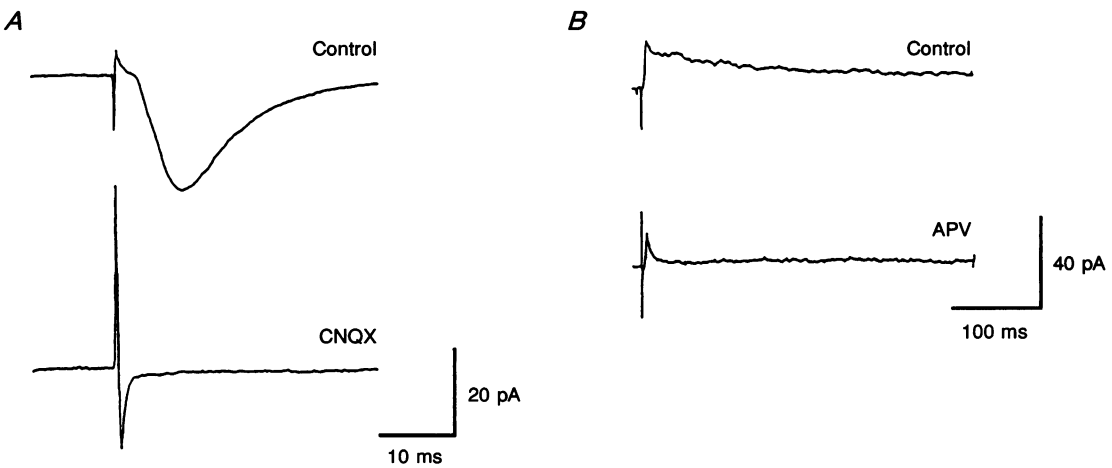

Figure 3. Pharmacological properties of unitary H-type EPSCs
Unitary H-type EPSCs were elicited in two different cells. *A*, H-type EPSCs evoked at −70 mV before and during application of CNQX (10 μM). *B*, H-type EPSCs evoked at +40 mV before and during application of APV (0·3 mM).

type 'S-type' EPSCs, since their amplitudes are small. S-type EPSCs probably involved both the non-NMDA and NMDA receptors, since they were apparently the dominant type of EPSC and since compound EPSCs were eliminated by CNQX and APV (see above). The contribution of NMDA receptors to individual S-type EPSCs, however, has not been systematically examined.

H-type EPSCs

We encountered another type of unitary EPSC in twelve experiments. In the example shown in Fig. 2, large EPSCs suddenly appeared at 12 V and remained unchanged up to 13 V (periods *b* and *d* in Fig. 2*A*). The amplitude histogram (Fig. 2*C*) has a clear peak at 47 pA, which is accompanied by a small component that peaks at 40 pA. The latency histogram (Fig. 2*E*) exhibits a sharp peak, suggesting that the EPSCs are monosynaptic and unitary. Interestingly, the times to peak of the EPSCs were rather large (Fig. 2*F*), and were clearly correlated with the amplitudes of the EPSCs in five out of twelve experiments (Fig. 2*G*). This appears to be due to asynchrony in the neurotransmitter release process, since we often detected broadening of the peak in large EPSCs (arrows in Fig. 2*B*). We will refer to unitary EPSCs of this type as 'H-type' EPSCs, since their amplitudes are huge compared with S-type EPSCs. H-type EPSCs involved both the non-NMDA and NMDA receptors, because the fast component was blocked by CNQX (Fig. 3*A*), and the slow component, which was

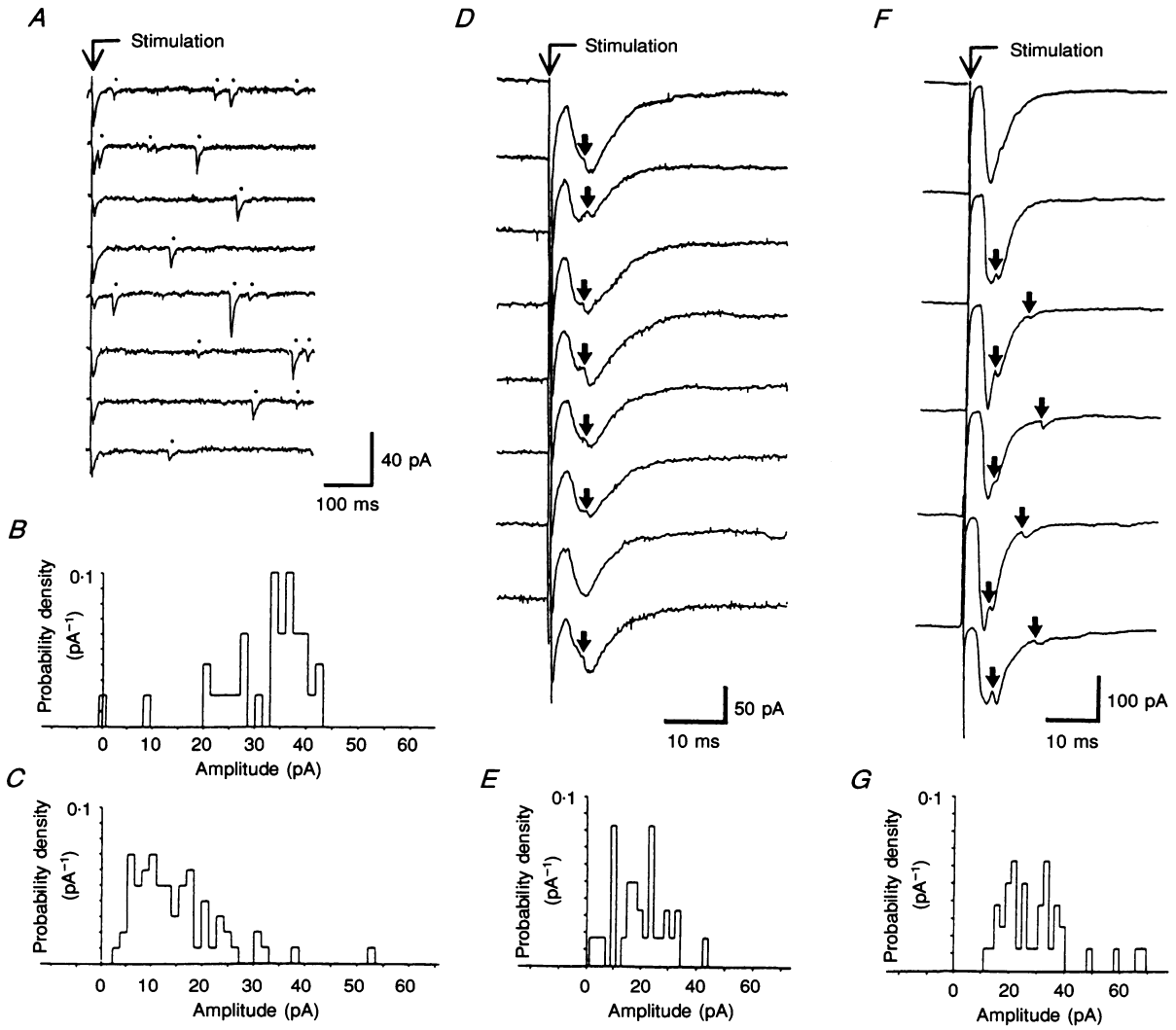

Figure 4. Spontaneous and polysynaptic activation of H-type EPSCs
A, spontaneous EPSCs induced during recording of unitary H-type EPSCs. Occurrences of spontaneous EPSCs are indicated by dots. *B* and *C*, amplitude histograms of evoked EPSCs (*B*; $n = 34$) and spontaneous EPSCs (*C*; $n = 69$). *D* and *F*, polysynaptic H-type EPSCs (arrows) evoked after the monosynaptic large EPSCs in two different cells. *E* and *G*, amplitude histograms of the polysynaptic EPSCs shown in *D* and *F*, respectively. *E*, $n = 31$; *G*, $n = 41$.

prominent at the depolarizing holding potential, was eliminated by APV (0·3 mM, Fig. 3*B*). The occurence of H-type EPSCs appeared not to depend much on the ages of rats between 9 and 12 days; we could detect H-type EPSCs mostly within five trials of repositioning of the stimulation pipettes.

Spontaneous H-type EPSCs were observed in five cells particularly during time periods when H-type synapses were stimulated (Fig. 4*A*). The presence of spontaneous H-type EPSCs supports the idea that evoked H-type EPSCs were due to stimulation of a single presynaptic fibre distinct from S-type EPSCs. Similarities in the time courses and amplitudes of the spontaneous EPSCs and evoked EPSCs (Fig. 4*A*) suggest that these spontaneous activities arise from the same synapse which generated the evoked H-type EPSCs. However, most of spontaneous EPSCs showed smaller amplitudes than evoked EPSCs (Fig. 4*C*), suggesting that the H-type EPSCs were composed of multiple quantal elements (Katz, 1969).

A distinction between S-type and H-type EPSCs was easily made, even during experiments, because the amplitudes of S-type EPSCs never exceeded 10 pA, while those of H-type EPSCs were often larger than 20 pA. Indeed, the mean amplitude of H-type EPSCs was 13 times larger than that of S-type EPSCs (Table 1). The threshold intensity of stimulation for H-type EPSCs was larger than that of S-type EPSCs (Table 1), suggesting that presynaptic fibres for H-type EPSCs are finer than those for S-type EPSCs. The times to peak of H-type EPSCs were slightly longer than that of S-type EPSCs (Table 1), reflecting the asynchronous release associated with H-type EPSCs. No significant difference was found in the latency and time constant (τ) of decay of EPSCs (Table 1). Both EPSCs could be evoked in the same neurone when a stimulation electrode was repositioned. We could detect unitary H-type EPSCs in nine out of twenty-one stimulation sites examined in three cells.

Table 1. Properties of unitary S-type and H-type EPSCs

	S-type EPSCs	H-type EPSCs
Threshold (V)	11·0 ± 0·88	14·3 ± 1·93*
Mean amplitude (pA)	2·05 ± 0·20	25·5 ± 2·57*
Failure	0·57 ± 0·06	0·24 ± 0·06*
Latency (ms)	4·09 ± 0·16	3·70 ± 0·23
Time to peak (ms)	2·45 ± 0·12	3.02 ± 0·28*
Decay τ (ms)	5·63 ± 0·39	6·04 ± 0·54
n	16	12

Asterisks indicate significant differences between the parameters of S-type and H-type EPSCs ($P < 0·05$). n represents number of cells examined.

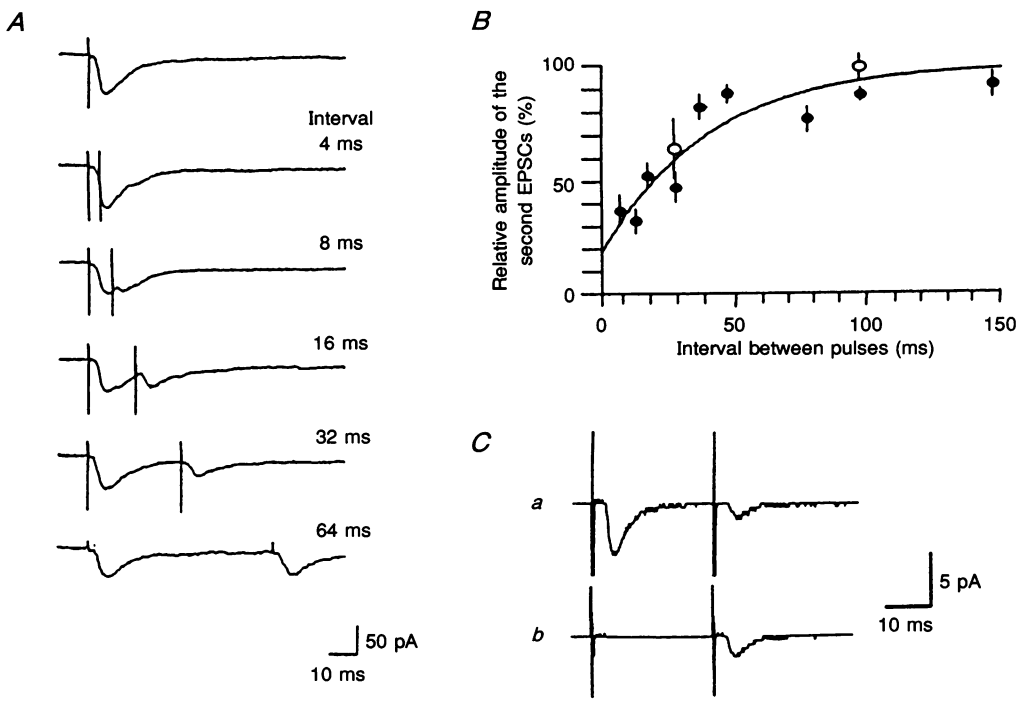

Figure 5. Paired-pulse depression of S-type EPSCs

A, depression of compound EPSCs evoked by two successive stimuli with varying intervals. *B*, amount of depression plotted against time. Circles represent mean values obtained from 5 or 6 experiments, and bars show S.E.M. ●, mean depression in the compound EPSCs. ○, mean depression of unitary S-type EPSCs obtained by averaging. The continuous line is the least-squares fit of the data with an exponential curve and a time constant of 39 ms. *C*, averaged current trace of S-type EPSCs showing the paired-pulse depression. Averaging was performed for all current traces in *a* ($n = 153$), but only for the current traces where the first EPSCs failed in *b* ($n = 83$).

Polysynaptic H-type EPSCs were often triggered following compound EPSCs triggered by stimuli strong enough to activate multiple fibres. Two examples are shown in panels *D* and *F* of Fig. 4, where late peaks with characteristic time courses for EPSCs appear between 3 and 15 ms after the onset of evoked EPSCs ($n = 6$, arrows in Fig. *4D* and *F*). Amplitudes of the late peaks were always large (Fig. *4E* and *G*) and fitted well with the amplitudes of H-type EPSCs. The late peak could not be accounted for by the miniature H-type EPSCs that appear more frequently after application of the stimuli. First, the delays in the appearances of the late peaks were fairly consistent (Fig. *4D*). Second, the late peak was never evoked by the weak stimuli which only stimulated single fibres. The late peak could also not have been caused by regenerative responses at the dendrites of medium spiny neurones, such as dendritic Ca^{2+} spikes, because it could be triggered even after the evoked EPSCs had mostly recovered to the baselines (the second arrow in Fig. *4F*). We therefore consider that the late peaks are due to polysynaptic activation of H-type EPSCs. The polysynaptic H-type EPSCs should have been generated by neurones close to the recorded cells, since evoked EPSCs as well as the late EPSCs were always sharply diminished when the stimulating electrodes were moved more than 200 μm away from the recorded cells. Stimulation of the cerebral cortex evoked no response in our horizontal slice preparations.

Paired-pulse depression of the two types of EPSCs

One of the known characteristics of EPSCs in striatal medium spiny neurones is paired-pulse depression: when a

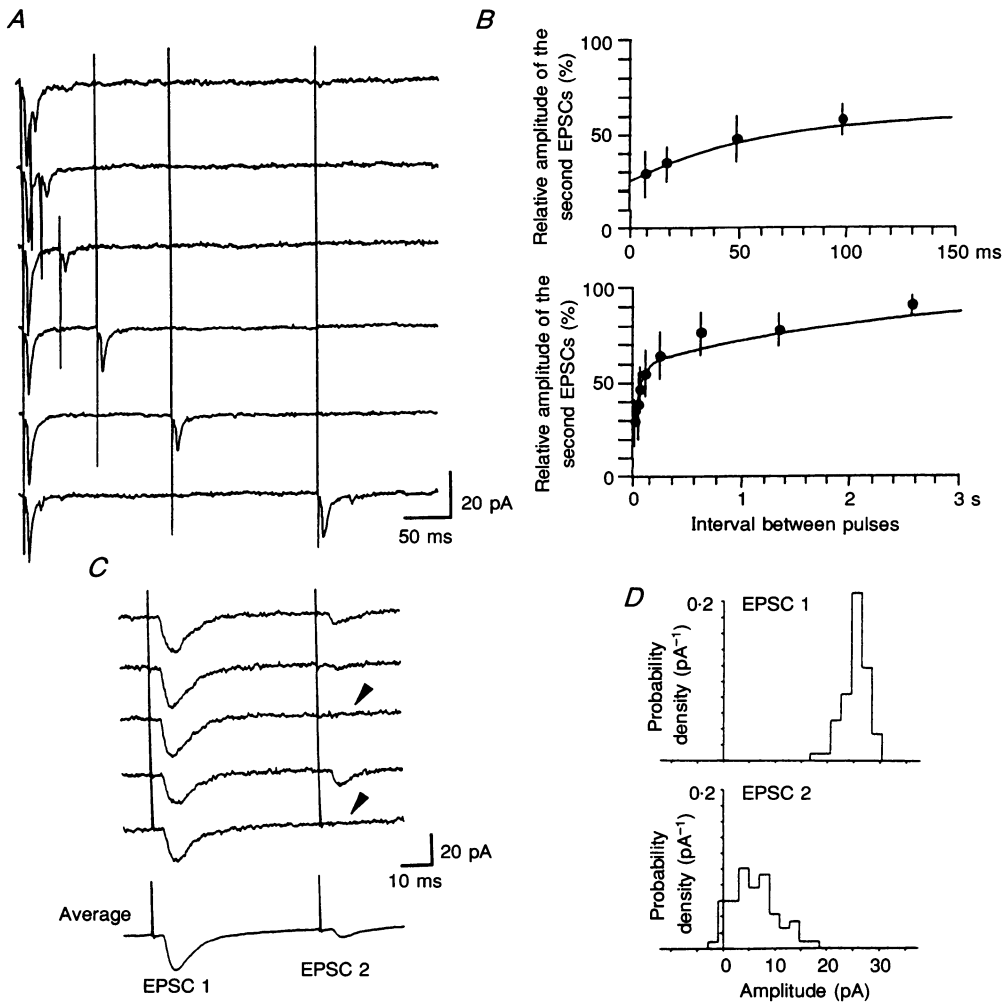

Figure 6. Paired-pulse depression of H-type EPSCs
A, depression of the unitary H-type EPSCs evoked by two successive stimuli with varying intervals. *B*, amount of depression plotted against intervals. ●, mean values from 5 separate experiments. The continuous line represent the least-squares fit of the data with double exponential functions having time constants of 58 and 2500 ms. *C*, five consecutive current traces for unitary H-type EPSCs, and averaged current traces of 62 traces. Arrowheads indicate occurrence of failure at the second stimuli. *D*, amplitude histograms for the first and second EPSCs ($n = 62$).

pair of stimuli is given, the amplitude of the second EPSC is smaller than that of the first (Lighthall, Park & Kitai, 1981; Wilson, Chang & Kitai, 1983). This paired-pulse depression was detected in most of the compound EPSCs that were evoked by stimulating multiple fibres (Fig. 5*A*). The mean amplitude of the second EPSCs evoked 30 ms after the first EPSCs was 50 % of the first EPSCs (Fig. 5*A*). The depression was most prominent when the interval was shortest, and was relieved rapidly with a time constant of 39 ms (Fig. 4*B*). These features of the paired-pulse depression of EPSCs appeared to reflect mainly those of unitary S-type EPSCs. Because similar degrees of the paired-pulse depression were detected in unitary S-type EPSCs after taking averages of consecutive traces (Fig. 5*Ca*). Relative amplitudes of the second EPSCs elicited at 30 ms varied between 50 and 100 % with a mean value of 65 % (○ in Fig. 5*B*). The inhibition was no longer detected when the second pulse was 100 ms after the first pulse (○ in Fig. 4*B*). It is important to note that the paired-pulse depression of the S-type EPSCs was still detected even when the first EPSCs failed. Figure 5*Cb* shows the averaged current trace obtained from the set of data shown in Fig. 5*Ca*, except that the averaging was selectively performed in the current traces whose first EPSCs were absent (a representative of 4 experiments). This strongly suggests that the depression involves presynaptic mechanisms, because the first stimulation did not cause activation of postsynaptic receptors.

The paired-pulse depression of unitary H-type EPSCs was always more long lasting. Figure 6*A* shows an example where the second EPSCs were suppressed to 40 % of control level at 30 ms and kept suppressed to 50 % of control level even at 150 ms. The time constant of recovery could be fitted with a sum of two exponentials with time constants of 58 ms and 2·5 s (Fig. 6*B*). The difference in the properties of the paired-pulse depression lends further support to the idea that the S-type and H-type EPSCs should originate from distinct synaptic inputs. A similar test of dependence of the second EPSCs on the first EPSCs (Fig. 5*D*) was not possible for the H-type EPSCs, since the first EPSCs failed less frequently. However, clear occurrence of the failures at the second stimulation (arrow heads in Fig. 6*C* and *D*) suggests that the depression of the H-type EPSCs also involves presynaptic mechanisms.

Paired-pulse depression was dependent on external Ca^{2+}. In experiments shown in Fig. 7, a pair of stimuli was triggered with an interval of 5 s, while the concentration of external Ca^{2+} was lowered to 0·25 mM. Ten consecutive traces were averaged to obtain mean levels of depression. The second S-type EPSCs were depressed by 50 % in control solution (Fig. 7*A a*), but were facilitated by 20 % in a low-Ca^{2+} solution (Fig. 7*A b*). Reduction of the depression was detected in eight out of eight experiments, and the facilitation was detected in three experiments. Similarly, the depression of the H-type EPSCs was lessened in the low-Ca^{2+} solution (Fig. 7*B*) in six out of six experiments, and facilitation was detected in one of them.

DISCUSSION

We have found that glutamatergic input to the striatal medium spiny neurones was classified into two types on the basis of its amplitude, presynaptic origin and paired-pulse depression (Fig. 8). We will first consider the origins of the two EPSCs, then discuss mechanisms of paired-pulse

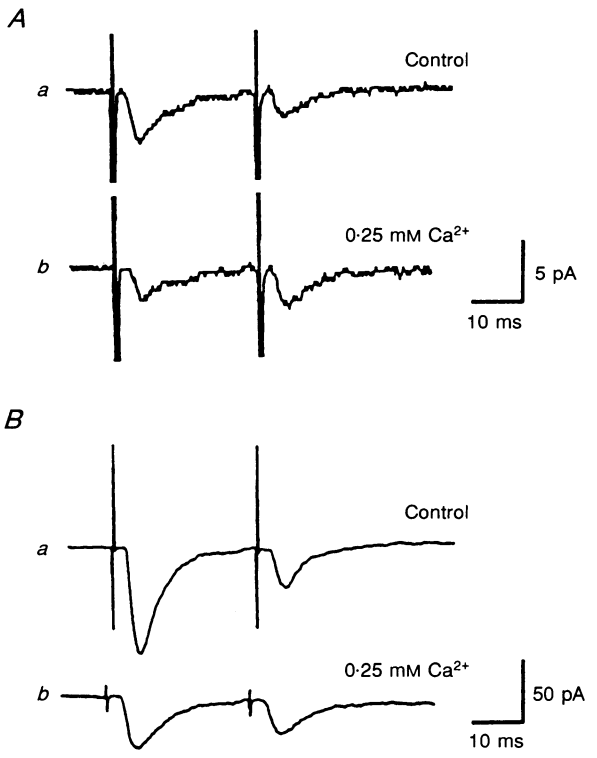

Figure 7. Ca^{2+} dependence of the paired-pulse depression
A and *B*, averaged current traces for unitary S-type EPSCs and H-type EPSCs, respectively, in control solution (*a*) and in low-Ca^{2+} solution (*b*).

depression, and finally speculate on a functional role for each type of EPSC.

S-type EPSCs

The majority of EPSCs evoked with focal stimulation in the striatum are considered as S-type. Indeed, the properties of paired-pulse depression of compound EPSCs were those of the S-type EPSCs. Since the cortex and thalamus supply predominantly glutamatergic inputs to the striatum, they should be the origin of S-type EPSCs. The small amplitude of S-type EPSCs is also consistent with anatomical features of afferent fibres from the cortex and thalamus in three respects. First, afferent fibres run straight in the striatum and form *en passant* synaptic contacts with the spine heads of the medium spiny neurones (Fox, Andrade, Hillman & Schwyn, 1971; Kemp & Powell, 1971). Therefore, each fibre could contact one medium spiny cell dendrite with only one synaptic bouton. Second, medium spiny neurones have relatively few dendritic trees and hence the chances of a straight axon meeting multiple dendrites of a medium spiny neurone should be low. Finally, the synaptic boutons of afferent fibres are relatively small, limiting the number of release sites (Kemp & Powell, 1971; Walmsley, 1991). Our results are also consistent with a previous electrophysiological study using adult rats, where each quantum of cortical afferent was too small to be resolved (Kawaguchi, Wilson & Emson, 1989).

H-type EPSCs

It is likely that H-type EPSCs are mediated by interneurones within the striatum, because H-type EPSCs could be polysynaptically activated by stimulation within the striatum (Fig. 4*B* and *C*). We consider that the late EPSCs are polysynaptic because they exhibited latencies at least 3 ms longer than monosynaptic EPSCs, and they needed stronger stimuli. More precisely, if the late EPSCs were monosynaptic, we could not explain why they always showed delays of more than 3 ms, because we stimulated the structures very close to the recorded neurones. Furthermore, if the late EPSCs were monosynaptic, the axons should be 900 μm long, as estimated using the slowest conduction velocity for thin unmyelinated axons (0·3 m s^{-1}). Since stimulation of the striatum more than 200 μm away from the recorded neurones failed to evoke any EPSCs, the axon would have to take a winding route within the confined areas. This type of axon collateral is reported for intrinsic neurones in the striatum, but not for cortical and thalamic afferents (Kemp & Powell, 1971). Therefore, the only candidate for the mother cell generating the late H-type EPSCs must be the intrinsic neurones (Fig. 8). However, we do not know for certain whether all H-type EPSCs do originate from the interneurones. Previous intracellular recordings from medium spiny neurones in the 'patch' area demonstrated that the EPSCs have a long latency and high threshold (Kawaguchi *et al.* 1989). Those authors also suggested the presence of excitatory neurones in the striatum, since there is a small amount of direct input from the neocortex to the patch area.

A clear asynchrony in release events was often detected (Fig. 2*B*). The asynchrony could be explained by assuming that the interneurones have long, unmyelinated and arborizing axons, which form multiple synaptic contacts with a medium spiny neurone (Fig. 8). If this is the case, stimulation of one branch of an axon will cause an action potential to propagate both orthodromically, to activate a bouton, and antidromically to invade other branches and activate other boutons. Conduction in such a long and

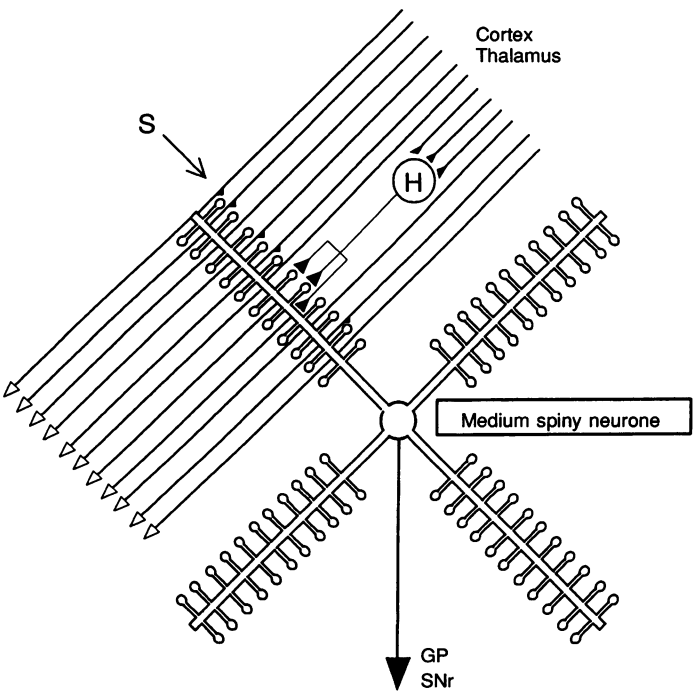

Figure 8. Schematic drawing of two glutamatergic synapses on the medium spiny neurone
Afferent fibres from cortex and thalamus may make an *en passant* synapse on a spine head of the medium spiny neurone (S), and generate small S-type EPSCs. One type of striatal intrinsic neurone, designated as H, generates huge H-type EPSCs. GP and SNr represent globus pallidus and substantia nigra pars reticulata, respectively.

unmyelinated axon could take a few milliseconds and could sometimes fail, which could account for the observed asynchrony (Fig. 2*B*) and the clear correlation between times to peak and peak amplitudes (Fig. 2*G*).

Calabresi, Mercuri & Bernardi (1990*a*,*b*) reported spontaneous depolarizing potentials (SDPs) in medium spiny neurones. SDPs have some features in common with spontaneous H-type EPSCs. First, SDPs were considered to be mediated by synaptic actions, since they were greatly diminished, but were not completely abolished, by TTX or in Ca^{2+}-free solution. The remaining small SDPs might correspond to miniature H-type EPSCs. Second, SDPs were not blocked by bicuculline, and hence were possibly mediated by glutamate. Third, the amplitudes of SDPs ranged between 2 and 15 mV, with an input resistance of about 25 MΩ (Calabresi *et al.* 1990*b*). A simple calculation using Ohm's law suggests that these correspond to inward currents with amplitudes of between 80 and 600 pA. The larger amplitudes of the SDPs could be due to the active membrane properties of the unclamped cells, such as dendritic Ca^{2+} spikes triggered by H-type EPSPs. Indeed, SDPs were voltage dependent, and were larger at depolarized holding potentials (Calabresi *et al.* 1990*a*). SDPs *in vivo* were capable of triggering action potentials by themselves in 35 % of the cells (Calabresi *et al.* 1990*a*).

One type of medium aspiny neurone could be a good candidate for the cell generating H-type EPSCs. It is generally accepted that the medium spiny neurones are GABAergic and the large aspiny neurones cholinergic (Graybiel, 1990). Therefore, they are unlikely to be glutamatergic as well. The remainder of neuronal types in the striatum are cumulatively referred to as medium aspiny neurones. In particularly, two types of medium aspiny neurones have been immunohistochemically identified. One is GABAergic (Bolam *et al.* 1983; Oertel & Mugnaini, 1984) and the other contains somatostatin and NO synthase (DiFiglia & Aronin, 1982; Vincent & Johansson, 1983; Takagi *et al.* 1983). In terms of neurotransmitters, therefore, the somatostatin-containing medium aspiny neurones seem to be the best candidates for the cells which generate H-type EPSCs. These neurones exhibit axon arborization, which would explain the multiquantal nature of H-type EPSCs. Preliminary experiments attempting to locate the interneurones with extracellular stimulating pipettes were not successful, due to the extensive mesh of axons covering every neurone in the striatum.

Paired-pulse depression

In most peripheral and CNS synapses, paired-pulse facilitation is regarded as a fundamental feature of synaptic transmission (Hovav, Parnas & Parnas, 1992). It is therefore of importance to consider why the EPSCs in the striatum showed depression instead, even in physiological conditions. Our results demonstrated that the depression of the two EPSCs was at least partly mediated by a presynaptic mechanism. This depression is presumably not due to presynaptic autoreceptors coupled with G-proteins, since there was no delay in the onset (Davies, Davies & Collingridge, 1990; Lamb & Pugh, 1992). Depletion of synaptic vesicles at the readily releasable pool is another possible mechanism for the synaptic depression (Glavinovic, 1991). This mechanism might account for the depression of the H-type EPSCs, because the amount of secretion at each EPSC appeared to be large. Interestingly, the climbing fibre inputs to cerebellar Purkinje cells also showed similar depression with slow recovery time (Konnerth, Llano & Armstrong, 1990). Depletion of synaptic vesicles alone, however, cannot account for the depression of the S-type EPSCs, because even without secretion during the first pulse, the second EPSCs were inhibited (Fig. 5*C*). The depression must therefore be mediated at some point before the fusion of synaptic vesicles. One explanation could be the presence of Ca^{2+}-dependent inhibitory mechanisms for vesicle fusion. The difference in the recovery time from depression in the two types of EPSCs may imply a difference in the underlying mechanisms.

Paired-pulse depression was reduced by lowering external Ca^{2+}, and the second EPSCs could be facilitated in low-Ca^{2+} solution. These results suggest that paired-pulse facilitation is also an intrinsic property of these EPSCs, as is the case for most other synapses, and it may be being masked by potent paired-pulse depression in the striatum. To our knowledge, there is no other type of synapse in the brain which displays greater paired-pulse depression than S-type and H-type EPSCs. There may be physiological reasons why paired-pulse facilitation is suppressed particularly in the striatum. One possibility is to allow the attenuation of temporal summation of EPSCs at specific synapses, which would necessitate the simultaneous occurrence of EPSCs for triggering action potentials. In any case, the difference in the extent of the depression in the two EPSCs may suggest distinct functional roles played by two glutamatergic synaptic inputs.

Nisenbaum and co-workers (Nisenbaum, Orr & Berger, 1988; Nisenbaum, Grace & Berger, 1992) have reported the presence of two types of neurones showing different properties in the paired-pulse depression. We have currently no idea how their two types of neurones could correlate with the types of neurones considered in this work (Fig. 8). The mechanisms of paired-pulse depression described by us and by Nisenbaum *et al.* (1992) must be different, because in their experiments depression was removed by blockage of $GABA_A$ receptors, while we studied depression in the presence of picrotoxin.

Our results are summarized in Fig. 8. These two separate input systems show some similarities with the two input systems in cerebellar Purkinje cells, where the parallel fibre inputs are small, and climbing fibre inputs are large and trigger Ca^{2+} spikes (Eccles *et al.* 1967). The climbing fibre EPSPs also showed paired-pulse depression (Konnerth *et al.* 1990). The difference in our study is that

the large input is not from extrinsic neurones in the cerebellum, but from intrinsic neurones in the striatum. It has been reported recently that excitatory synapses to the medium spiny neurones undergo long-term modification after tetanic stimulation (Calabresi, Maj, Mercuri & Bernardi, 1992*a*; Calabresi, Maj, Pisani, Mercuri & Bernardi, 1992*b*; Calabresi, Pisani, Mercuri & Bernardi, 1992*c*; Tyler, Lovinger & Merritt, 1992). It could therefore be speculated that the presynaptic axons which generate H-type EPSCs may play a role analogous to climbing fibres in Purkinje cells, giving error or teacher signals (Marr, 1969; Albus, 1977; Ito, 1984). The presence of two distinct excitatory inputs to the medium spiny neurones should thus be taken into account in the future whenever the operation of striatal neuronal circuits is considered.

REFERENCES

Albus, J. S. (1971). A theory of cerebellar function. *Mathematical Bioscience* **10**, 25–61.

Bolam, J. P., Clark, D. J., Smith, A. D. & Somogyi, P. (1983). A type of aspiny neuron in the rat neostriatum accumulates [^{3}H]gamma-aminobutyric acid: Combination of Golgi staining, autoradiography and electron microscopy. *Journal of Comparative Neurology* **213**, 121–134.

Bolam, J. P., Wainer, B. H. & Smith, A. D. (1984). Characterization of cholinergic neurones in the rat neostriatum. A combination of choline acetyltransferase immunocytochemistry, Golgi impregnation and electron microscopy. *Neuroscience* **12**, 711–712.

Calabresi, P., Maj, R., Mercuri, N. B. & Benardi, G. (1992*a*). Coactivation of D1 and D2 dopamine receptors is required for long-term synaptic depression in the striatum. *Neuroscience Letters* **142**, 95–99.

Calabresi, P., Maj, R., Pisani, A., Mercuri, N. B. & Bernardi, G. (1992*b*). Long-term synaptic depression in the striatum: physiological and pharmacological characterization. *Journal of Neuroscience* **12**, 4224–4233.

Calabresi, P., Mercuri, B. & Bernardi, G. (1990*a*). Synaptic and intrinsic control of membrane excitability of neostriatal neurons. I. An in vivo analysis. *Journal of Neurophysiology* **63**, 651–662.

Calabresi, P., Mercuri, B. & Bernardi, G. (1990*b*). Synaptic and intrinsic control of membrane excitability of neostriatal neurons. II. An in vitro analysis. *Journal of Neurophysiology* **63**, 663–675.

Calabresi, P., Pisani, A., Mercuri, N. B. & Bernardi, G. (1992*c*). Long-term potentiation in the striatum is unmasked by removing the voltage-dependent magnesium block of NMDA receptor channels. *European Journal of Neuroscience* **4**, 929–935.

Davies, C. H., Davies, S. N. & Collingridge, G. L. (1990). Paired-pulse depression of monosynaptic GABA-mediated inhibitory postsynaptic responses in rat hippocampus. *Journal of Physiology* **424**, 513–531.

DiFiglia, M. & Aronin, N. (1982). Ultrastructural features of immunoreactive somatostatin neurons in the rat caudate-nucleus. *Journal of Neuroscience* **2**, 1267–1274.

Eccles, J. C., Ito, M. & Szentágothai, J. (1967). *The Cerebellum as a Neuronal Machine*. Springer-Verlag, New York, Heidelberg.

Edwards, F. A., Konnerth, A., Sakmann, B. & Takahashi, T. (1989). A thin slice preparation for patch clamp recordings from neurones of the mammalian central nervous system. *Pflügers Archiv* **414**, 600–612.

Edwards, F. A., Konnerth, A. & Sakmann, B. (1990). Quantal analysis of inhibitory synaptic transmission in the dentate gyrus of rat hippocampal slices: A patch-clamp study. *Journal of Physiology* **430**, 213–249.

Fox, C. A., Andrade, A. N., Hillman, D. E. & Schwyn, R. C. (1971). The spiny neurons in the primate striatum: A Golgi and electron microscopic study. *Journal für Hirnforshung* **13**, 181–201.

Gerfen, C. R. (1992). The neostriatal mosaic: Multiple levels of compartmental organization in the basal ganglia. *Annual Review in Neuroscience* **15**, 285–320.

Glavinovic, M. I. (1991). Origin of synaptic depression. *Periodicum Biologorum* **93**, 519–524.

Graybiel, A. M. (1990). Neurotransmitters and neuromodulators in the basal ganglia. *Trends in Neurosciences* **13**, 244–254.

Hovav, G., Parnas, H. & Parnas, I. (1992). Neurotransmitter release: facilitation and three-dimentional diffusion of intracellular calcium. *Bulletin of Mathematical Biology* **54**, 875–894.

Ito, M. (1984). *The Cerebellum and Neural Control*. Raven Press, New York.

Jiang, Z. G. & North, R. A. (1991). Membrane properties and synaptic responses of rat striatal neurones *in vitro*. *Journal of Physiology* **443**, 533–553.

Katz, B. (1969). *The Release of Neural Transmitter Substances*. Liverpool University Press, Liverpool.

Kawaguchi, Y., Wilson, C. J. & Emson, P. C. (1989). Intracellular recording of identified neostriatal patch and matrix spiny cells in a slice preparation preserving cortical inputs. *Journal of Neurophysiology* **62**, 1052–1068.

Kemp, J. M. & Powell, T. P. S. (1971). The structure of the caudate nucleus of the cat: Light and electron microscopy. *Philosophical Transactions of the Royal Society* B **262**, 383–401.

Konnerth, A., Llano, I. & Armstrong, C. M. (1990). Synaptic currents in cerebellar Purkinje cells. *Proceedings of National Academy of Sciences of the USA* **87**, 2662–2665.

Lamb, T. D. & Pugh, E. N. (1992). G-protein cascades: gain and kinetics. *Trends in Neurosciences* **15**, 291–298.

Lighthall, J. W., Park, M. R. & Kitai, S. T. (1981). Inhibition in slices of rat neostriatum. *Brain Research* **212**, 182–187.

Marr, D. (1969). A theory of cerebellar cortex. *Journal of Physiology* **202**, 437–470.

Mori, A., Takahashi, T., Miyashita, Y. & Kasai, H. (1992). Quantal analysis of single presynaptic boutons of glutamatergic synapses in thin slices from rat neostriatum. *Neuroscience Research Supplement* **17**, s77.

Neher, E. (1992). Correction for liquid junction potentials in patch clamp experiments. *Methods in Enzymology* **207**, 123–130.

Nisenbaum, E. S., Orr, W. B. & Berger, T. W. (1988). Evidence for two functionally distinct subpopulations of neurons within the rat striatum. *Journal of Neuroscience* **8**, 4138–4150.

Nisenbaum, E. S., Grace, A. A. & Berger, T. W. (1992). Functionally distinct subpopulations of striatal neurons are differentially regulated by GABAergic and dopaminergic inputs – II. In vitro analysis. *Neuroscience* **48**, 579–593.

Oertel, W. H. & Mugnaini, E. (1984). Immunocytochemical studies of GABAergic neurons in rat basal ganglia and their relations to other neuronal systems. *Neuroscience Letters* **47**, 233–238.

Takagi, H., Somogyi, P., Somogyi, J. & Smith, A. D. (1983). Fine structural studies of a type of somatostatin-immunoreactive neurons and its synaptic connections in the rat neostriatum: A correlated light and electron microscopic study. *Journal of Comparative Neurology* **214**, 1–16.

Tyler, E. C., Lovinger, D. M. & Merritt, A. (1992). Short- and long-term synaptic depression in the neostriatum. *Society for Neuroscience Abstracts* **18**, 1351.

VINCENT, S. R. & JOHANSSON, O. (1983). Striatal neurons containing both somatostatin and avian pancreatic polypeptide (APP)-like immunoreactivities and NADPH diaphorase activity: A light and electron microscopic study. *Journal of Comparative Neurology* **217**, 252–263.

WALMSLEY, B. (1991). Central synaptic transmission: Studies at the connection between primary afferent fibers and dorsal spinocerebellar tract (DSCT) neurones in Clarke's column of the spinal cord. *Progress in Neurobiology* **36**, 391–423.

WILSON, C. J., CHANG, H. T. & KITAI, S. T. (1983). Disfacilitation and long-lasting inhibition of neostriatal neurons in the rat. *Experimental Brain Research* **51**, 227–235.

Acknowledgements

The authors thank Tristan Davies and George J. Augustine for improving the manuscript. This work was supported by Grants-in-Aid for Scientific Research from the Japanese Ministry of Education, Science and Culture to H.K., by a Grant for Scientific Research on Priority Areas from the Japanese Ministry of Education, Science and Culture to Y.M., and by a Research Grant from the Human Frontier Science Program to H.K.

Author's present address

A. Mori: Pharmaceutical Research Laboratories, Kyowa Hakko Kogyo Co. Ltd, Nagaizumi-cho, Sunto-gun, Shizuoka 411, Japan.

Received 12 May 1993; revised 9 September 1993; accepted 22 September 1993.